Bull. Astr. Soc. India (1989) 17, 14–26

Effects of aberration and advection in a partially scattering medium

A. Peraiah and M. Srinivasa Rao *Indian Institute of Astrophysics, Bangalore 560 034*

Received 1989 January 2; accepted 1989 January 28

Abstract. We have investigated the effects of aberration and advection terms, which are of order v/c (where v is the velocity of gas and c is the velocity of light) on the solution of the radiative transfer equation. We have employed a plane-parallel medium which is moving with velocities 1000, 2000, 3000, 4000 or 5000 km s^{-1} ($\beta = 0.0033 - 0.07$ where $\beta = v/c$). The calculations have been done in the fluid frame, with monochromatic radiation field. We introduce emission sources inside the medium. We assume equal contribution from internal emission and from isotropic and coherent scattering to the radiation field. We have estimated the effects of aberration and advection on the mean intensities and on outward fluxes for different velocities and different optical depths. The effects are found in terms of the mean intensity $\bar{J}\{= [J(v = 0) - J(v > 0)] \times 100/J(v = 0)\}$ and the outward flux $\bar{F}\{= [F(v = 0) - F(v > 0)] \times 100/F(V = 0)\}$. We set ω (albedo for single scattering) equal to 0.5 and the Planck function equal to $B(n) = 1$ (case i) and $B(n) \sim 1/n^2$ (case ii). In case (i), the values of $\bar{J}$ and $\bar{F}$ are not spectacular and the maximum changes are in the range of 2 to 3%. In case (ii) the changes are in the range of 5 to 6%.

Key words : radiative transfer — aberration — advection

1. Introduction

The effects of aberration and advection generated in a fast moving fluid have been examined in an earlier paper (Peraiah 1987 ≡ paper 1) where we have considered a medium scattering isotropically and coherently and no internal sources were considered. In a scattering medium, we found that the radiation field changes are quite considerable. The high velocities coupled with large scattering optical depths generate radiation fields which are totally different from those generated by the low velocity media. We have to find out the effects of aberration and advection on emitting medium which is moving fast.

In this paper we solved the time-independent radiative transfer equation in the fluid frame in which the scattering and absorption by the medium takes place. We retain the terms of the order of v/c. We solve the equation of radiative transfer with coherent isotropic scattering medium stratified in plane parallel layers.

2. Formulation of the problem

The monochromatic, plane-parallel, time-independent radiative transfer equation in fluid frame (Castor 1972; paper 1) with aberration and advection terms is given by

$$(\mu + \beta)\frac{\partial I(z, \mu)}{\partial z} + \frac{\mu(\mu^2 - 1)}{c}\frac{\partial v}{\partial z}\frac{\partial I(z, \mu)}{\partial \mu} + \frac{3\mu^2}{c}\frac{\partial v}{\partial z} I(z, \mu)$$
$$= K[S - I(z, \mu)], \qquad \text{...(1)}$$

where $\mu = (\mu' - \beta)/(1 - \mu'\beta)$ and μ' $(0 < \mu' < 1)$ is the cosine of the angle made by the ray with z-axis; $\beta = v/c$; $I(z, \mu)$ is the specific intensity of the ray; K is the absorption coefficient. S is the source function given by

$$S = [1 - \omega(z)]\, B(z) + \tfrac{1}{2}\,\omega(z) \int_{-1}^{+1} P(z, \mu_1', \mu_2')\, I(z, \mu_2')\, d\mu_2', \qquad \text{...(2)}$$

where $\omega(z)$ is the albedo for single scattering. We set $\omega = 0.5$ in all cases. $B(z)$ is the Planck function; $P(z, \mu_1', \mu_2')$ is the phase function for isotropic scattering.

We integrate equation (1) together with the source function given in equation (2) as described in paper 1.

We shall briefly describe the solution for a reader who is not familiar with this approach. Equation (1) is written after integration over $z - \mu$ grid as follows :

$$\frac{2}{\Delta z}(\bar{\mu} + \beta)\, I_z + (g + \bar{\mu}\cdot\Delta\,\mu)\frac{d\beta}{dz} I_\mu + \frac{1}{3}\Delta\,\mu\, I_{z\mu}$$
$$+ \left(K + 3\bar{\mu}^2\frac{d\beta}{dz}\right) I_0 = KS_0, \qquad 0 < \mu \leqslant 1, \qquad \text{...(3)}$$

and

$$\frac{2}{\Delta z}(\beta - \bar{\mu})\, I_z + g(+ \bar{\mu}\cdot\Delta\mu)\frac{d\beta}{dz} - \frac{1}{3} I_{z\mu}\,\Delta\mu + \left(K + 3\bar{\mu}^2\frac{d\beta}{dz}\right) = KS,$$
$$0 > \mu > -1. \qquad \text{...(4)}$$

Here $d\beta/dz$ is constant over the interval (z_1, z_{1-1}) and

$$\bar{\mu}^2 = (\bar{\mu})^2 + \frac{1}{12}(\Delta\mu)^2, \qquad \text{...(5)}$$

$$g = \frac{2\bar{\mu}}{\Delta\mu}(<\mu^2> - 1), \qquad \text{...(6)}$$

$$<\mu^2> = \frac{1}{2}(\mu_j^2 + \mu_{j-1}^2), \qquad \text{...(7)}$$

$$\bar{\mu} = \tfrac{1}{2}(\mu_j + \mu_{j-1}), \quad ...(8)$$

$$\Delta\mu = (\mu_j - \mu_{j-1}), \quad ...(9)$$

$$\bar{z} = \tfrac{1}{2}(z_i - z_{i-1}), \quad ...(10)$$

$$\Delta z = (z_i - z_{i-1}), \quad ...(11)$$

where z_i, z_{i-} and μ_j, μ_{j-1} are the discrete points along the $z - \mu$ grid. I_0, I_z, I_μ, $I_{z\mu}$ are the interpolation coefficients given by

$$I = I_0 + \xi\, I_z + \eta\, I_\mu + \xi\eta\, I_{z\mu} \quad ...(12)$$

with

$$\xi = \frac{z - \bar{z}}{\Delta z/2} \text{ and } = \frac{\mu - \bar{\mu}}{\Delta\mu/2}. \quad ...(13)$$

We now replace these interpolation coefficients by their nodal values. Then, equations (3) and (4) can be rewritten as

$$A_a I_{j-1}^{i-1,+} + A_b I_j^{i-1,+} + A_c I_{j-1}^{i,+} + A_d I_j^{i,+}$$
$$= \tau \left[S_{j-1}^{i-1,+} + S_j^{i-1,+} + S_{j-1}^{i,+} + S_j^{i,+} \right] \quad ...(14)$$

and

$$A'_a I_{j-1}^{i-1,-} + A'_b\, I_j^{i-1,-} + A'_c\, I_{j-1}^{i,-} + A'_d\, I_j^{i,-}$$
$$= \tau \left[S_{j-1}^{i-1,-} + S_j^{i-1,-} + S_{j-1}^{i,-} + S_j^{i,-} \right], \quad ...(15)$$

where

$$A_a = \tau + a_1 + b_1 - c_1, \quad ...(16)$$

$$A_b = \tau - a_1 + b_2 - c_1, \quad ...(17)$$

$$A_c = \tau - a_2 + b_1 + c_1, \quad ...(18)$$

$$A_d = \tau + a_2 + b_2 + c_1, \quad ...(19)$$

$$A'_a = \tau - a_2 + b_1 - c_2, \quad ...(20)$$

$$A'_b = \tau + a_2 + b_2 - c_2, \quad ...(21)$$

$$A'_c = \tau + a_1 + b_1 + c_2, \quad ...(22)$$

$$A'_d = \tau - a_2 + b_2 + c_2, \quad ...(23)$$

$$a_1 = \Delta\mu(\tfrac{1}{3} - \bar{\mu}\cdot\Delta\beta), \quad ...(24)$$

$$a_2 = \Delta\mu(\tfrac{1}{3} + \bar{\mu}\cdot\Delta\beta), \quad ...(25)$$

$$b_1 = \Delta\beta(3\bar{\mu}^2 - g), \quad ...(26)$$

$$b_2 = \Delta\beta(3\bar{\mu}^2 + g), \quad ...(27)$$

$$c_1 = 2(\beta + \bar{\mu}), \quad ...(28)$$

$$c_2 = 2(\beta - \bar{\mu}), \quad \text{...(29)}$$

$$\Delta\beta = (\beta_{n+1} - \beta_n), \quad \text{...(30)}$$

$$I_{j-1}^{i-1,+} = I(z_{i-1}, +\mu_{j-1}) \text{ etc.}, \quad \text{...(31)}$$

$$S_{j-1}^{i-1,+} = \sum \frac{\omega}{2} (P^{++} CI^{i-1,+} + P^{+-} CI^{i-1,-})_{j-1} + (1-\omega) B^{+}. \quad (32)$$

$S_{j-1}^{i-1,-}$, $S_j^{i,+}$ etc. can be similarly written. τ is the optical depth given by

$$\Delta\tau = K \cdot \Delta z. \quad \text{...(33)}$$

Equations (14) and (15) can be rewritten for the J-angles

$$(\mathbf{A}^{cd} - \tau\mathbf{Q}\mathbf{\Gamma}^{++})\,\mathbf{I}_i^{+} + (\mathbf{A}^{ab} - \tau\mathbf{Q}\mathbf{\Gamma}^{++})\,\mathbf{I}_{i-1}^{+} = \tau\mathbf{Q}\mathbf{\Gamma}^{+-}\mathbf{I}_i^{-} + \tau\mathbf{Q}\mathbf{\Gamma}^{+-}\mathbf{I}_{i-1}^{-} \quad \text{...(34)}$$

and

$$(\mathbf{A}'^{cd} - \tau\mathbf{Q}\mathbf{\Gamma}^{--})\,\mathbf{I}_i^{-} + (\mathbf{A}'^{ab} - \tau\mathbf{Q}\mathbf{\Gamma}^{--})\,\mathbf{I}_{i-1}^{-} = \tau\mathbf{Q}\mathbf{\Gamma}^{-+}\,\mathbf{I}_i^{+} + \tau\mathbf{Q}\mathbf{\Gamma}^{-+}\,\mathbf{I}_{i-1}^{+}, \quad \text{...(35)}$$

where

$$\{Q_{jj}, Q_{j,j+1}\} = 1, \quad (36)$$

$$\mathbf{A}^{ab} = \begin{bmatrix} A_a^{j-1} & A_b^{j} & & \\ & A_a^{j} & A_b^{j+1} & \\ & & A_a^{J-1} & A_b^{J} \\ & & & A_a^{J} \end{bmatrix}. \quad \text{...(37)}$$

Other matrices $\mathbf{A}^{cd}$, $\mathbf{A}'^{ab}$, $\mathbf{A}'^{cd}$ are similarly defined.

$$\mathbf{\Gamma}^{++} = \tfrac{1}{2}\,\mathbf{P}^{++}\,\mathbf{C} \text{ etc}, \quad \text{...(38)}$$

$$\mathbf{P}^{++} = \mathbf{P}(+\mu_1, +\mu_2), \quad \text{...(39)}$$

C's are the quadrature weights of the angle integration. We derive the transmission and reflection operators as described in Peraiah & Varghese (1985):

$$\mathbf{t}(i, i-1) = \mathbf{R}^{+-}[\mathbf{\Delta}^{+}\mathbf{A} + \mathbf{r}^{+-}\mathbf{\Delta}^{-}\mathbf{C}], \quad \text{...(40)}$$

$$\mathbf{t}(i-1, i) = \mathbf{R}^{-+}[\mathbf{\Delta}^{-}\mathbf{D} + \mathbf{r}^{-+}\mathbf{\Delta}^{+}\mathbf{B}], \quad \text{...(41)}$$

$$\mathbf{r}(i, i-1) = \mathbf{R}^{-+}[\mathbf{\Delta}^{-}\mathbf{C} + \mathbf{r}^{-+}\mathbf{\Delta}^{+}\mathbf{A}], \quad \text{...(43)}$$

$$\mathbf{r}(i-1, i) = \mathbf{R}^{+-}[\mathbf{\Delta}^{+}\mathbf{B} + \mathbf{r}^{-+}\mathbf{\Delta}^{-}\mathbf{D}], \quad \text{...(43)}$$

$$\mathbf{\Delta}^{+} = [\bar{A}_{cd} - \tau\mathbf{\Gamma}^{++}]^{-1}, \quad \text{...(44)}$$

$$\mathbf{\Delta}^{-} = [\bar{A}_{ab} - \tau\mathbf{\Gamma}^{--}]^{-1}, \quad \text{...(45)}$$

$$\bar{\mathbf{A}}_{ab} = \mathbf{Q}^{-1}\,\bar{\mathbf{A}}^{ab}, \qquad \ldots(46)$$

$$\bar{\mathbf{A}}'_{ab} = \mathbf{Q}^{-1}\,\bar{\mathbf{A}}'_{cd}, \qquad \ldots(47)$$

$$\bar{\mathbf{A}}_{cd} = \mathbf{Q}^{-1}\,\bar{\mathbf{A}}^{cd}, \qquad \ldots(48)$$

$$\bar{\mathbf{A}}'_{ab} = \mathbf{Q}^{-1}\,\bar{\mathbf{A}}'_{ab}, \qquad \ldots(49)$$

$$\mathbf{r}^{+-} = \tau\boldsymbol{\Delta}^{+}\,\boldsymbol{\Gamma}^{+-}, \qquad \ldots(50)$$

$$\mathbf{A} = \tau\boldsymbol{\Gamma}^{++} - \bar{\mathbf{A}}_{ab}, \qquad \ldots(51)$$

$$\mathbf{B} = \tau\boldsymbol{\Gamma}^{+-}, \qquad \ldots(52)$$

$$\mathbf{C} = \tau\boldsymbol{\Gamma}^{-+}, \qquad \ldots(53)$$

$$\mathbf{D} = \tau\boldsymbol{\Gamma}^{++} - \bar{\mathbf{A}}'_{cd}, \qquad \ldots(54)$$

$$\mathbf{R}^{+-} = [\mathbf{I} - \mathbf{r}^{+-}\,\mathbf{r}^{-+}]^{-1}. \qquad \ldots(55)$$

The quantities $\mathbf{r}^{-+}$, $\mathbf{R}^{-+}$ are obtained by interchanging the signs + and − in $\mathbf{r}^{+-}$ and $\mathbf{R}^{+-}$.

We have calculated the radiation field through these operators as described in Peraiah & Varghese (1985).

3. Discussion of the results

We present the results in figures 1–14. We have considered a plane parallel slab bounded by $\tau = \tau_{max}$ and $\tau = 0$ and divided into N layers.

$$I^{-}(\tau = \tau_{max}, \mu_j) = 0, \qquad \ldots(56)$$

$$I^{+}(\tau = 0, \mu_j) = 0, \qquad \ldots(57)$$

where τ is the optical depth. These boundary conditions imply that there is no radiation incident on either side of the medium. Radiation is transferred because of the presence of emission from the medium itself. These sources are represented by a predefined Planck function B. Two cases of variation of the Planck function are (i) $B = 1$ and (ii) $B \sim 1/n^2$. Our aim is to find out how variations in emission source affect the radiation field when advection and aberration are included.

We assume that at the bottom of the atmosphere the medium is at rest and that the velocity is increasing radially, that is,

$$v(\tau = \tau_{max}) = 0, \qquad \ldots(58)$$

$$v(\tau = 0) = v, \qquad \ldots(59)$$

where v varies in steps of 1000 km s^{-1}, from 0 to 5000 km s^{-1}, corresponding to β = 0.00670, 0.0033, 0.0067, 0.01, 0.013, 0.0167.
The velocity gradient is constant with $dv/d\tau < 0$.

Mean intensities and outward fluxes are computed from

$$J = \tfrac{1}{2} \int_{-1}^{+1} I(\mu)\, d\mu \qquad \text{...(60)}$$

and

$$F = \int_0^1 I(\mu)\ \mu\ d\mu. \qquad \text{...(61)}$$

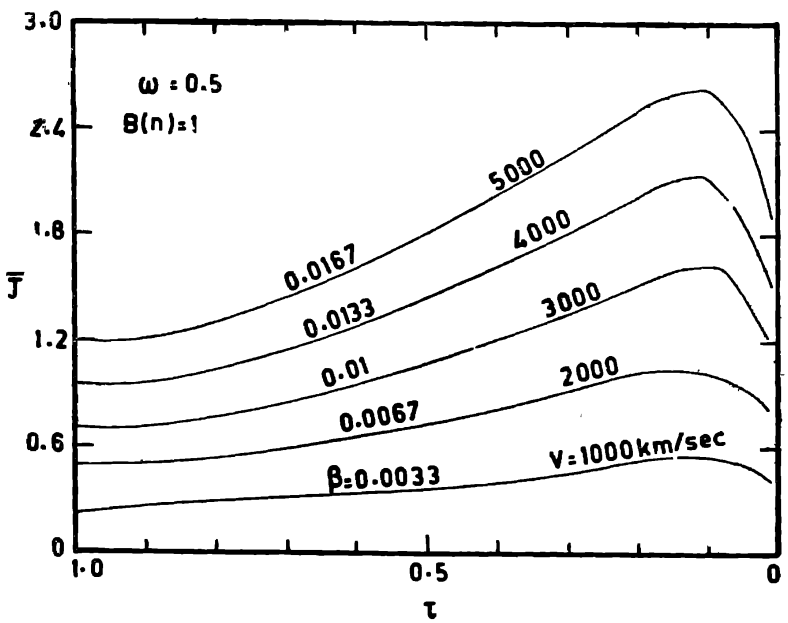

Figure 1. The changes in mean intensities J are plotted for the optical depth = 1. $\tau = 0$ corresponds to the emergent intensities. These curves correspond to the values of the expansion velocities $V = 1000$, 2000, 3000, 4000, 5000 km s^{-1}. The Planck function is assumed to be uniform throughout the medium. The albedo for single scattering $\omega = 0.5$.

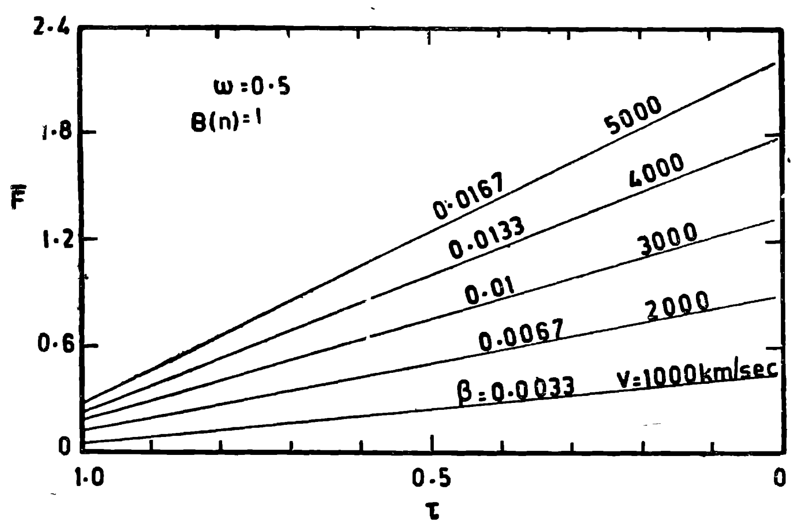

Figure 2. The differences in the outward fluxes for a total optical depth $\tau = 1$ are shown for the same values of the velocities, Planck function and albedo for single scattering as employed in figure 1.

We wish to estimate the change in radiation field emitted by the medium in motion and at rest. The quantities $\bar{J}$ and $\bar{F}$ are defined by

$$\bar{J} = \frac{J(v = 0) - J(v > 0)}{J(v = 0)} \times 100 \qquad \ldots(62)$$

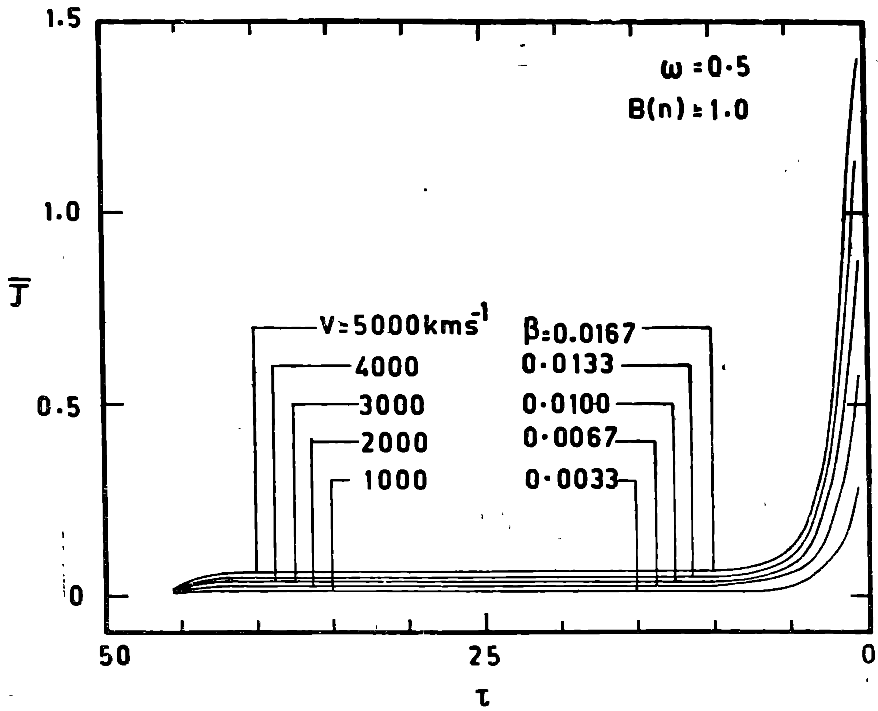

Figure 3. Same as those given in figure 1 for a total optical depth of 50.

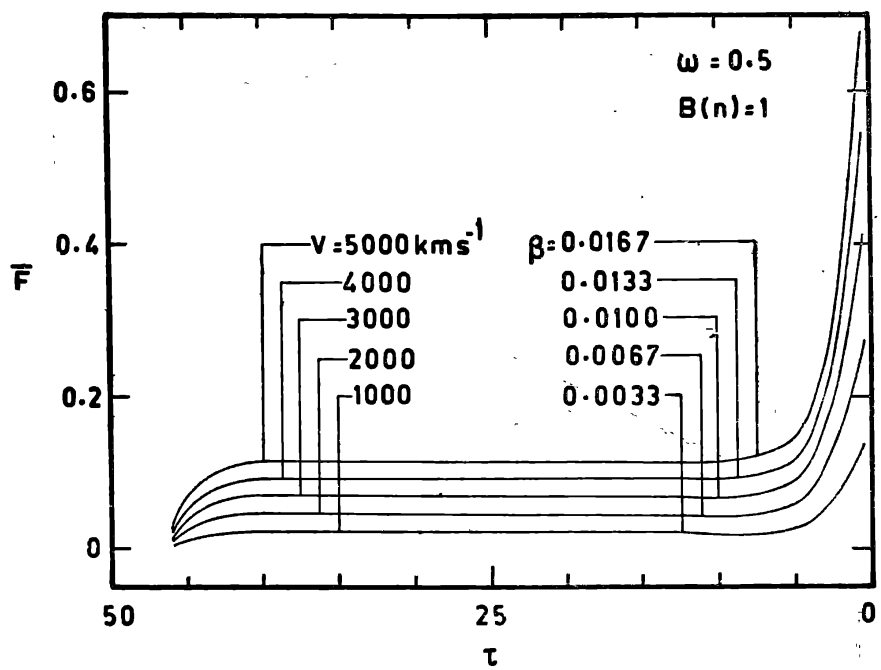

Figure 4. Same as those given in figure 2 for a total optical depth of 50.

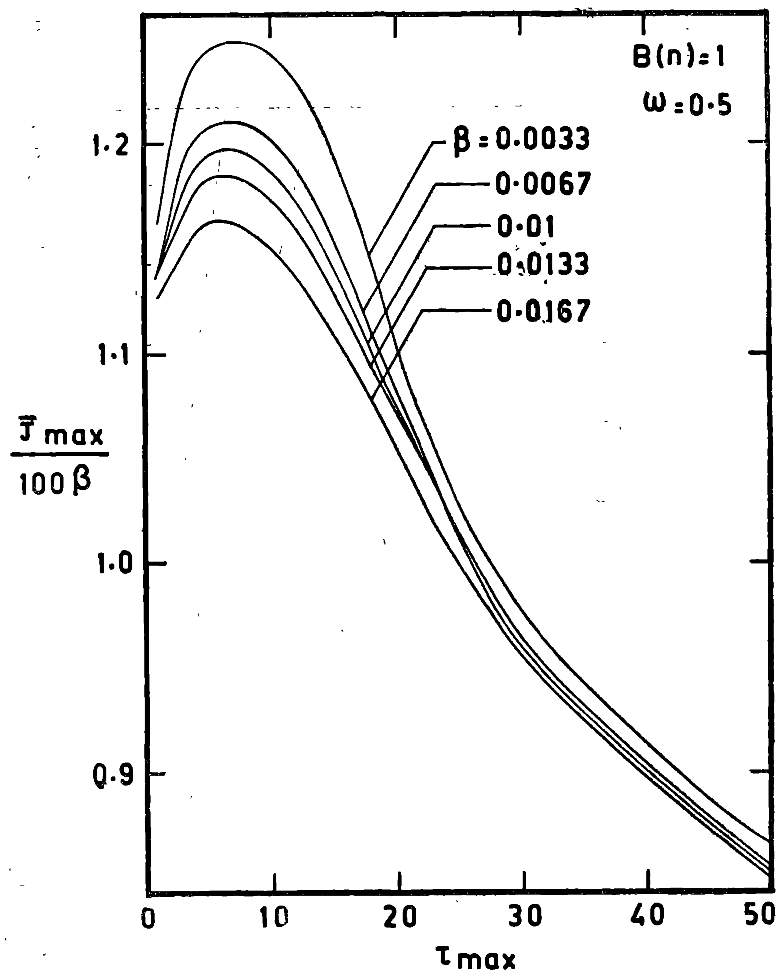

Figure 5. The amplification factors for the mean intensities are plotted for all the velocities.

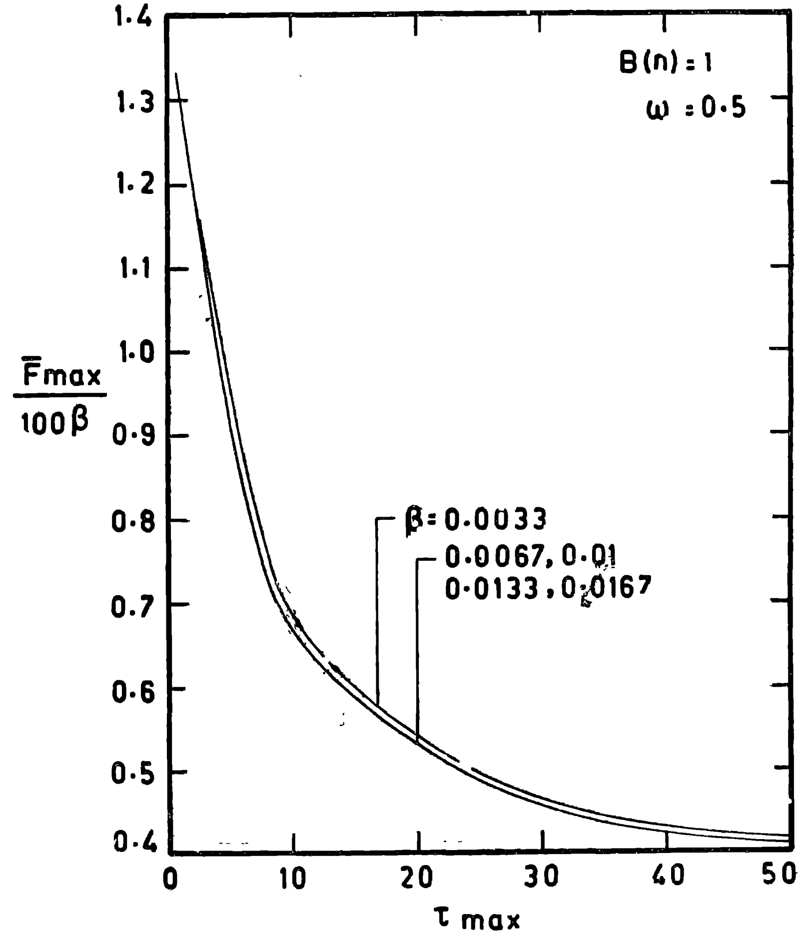

Figure 6. The amplification factor of outward fluxes are plotted for the different velocities.

$$\bar{F} = \frac{F(v = 0) - F(v > 0)}{F(v = 0)} \times 100. \qquad \ldots(63)$$

We employed four angle points on $\mu \in [0, 1]$ ($\mu_1 = 0$, $\mu_2 = 0.2764$, $\mu_3 = 0.7236$, $\mu_4 = 1$). The medium is divided into 100 layers of equal geometrical thickness

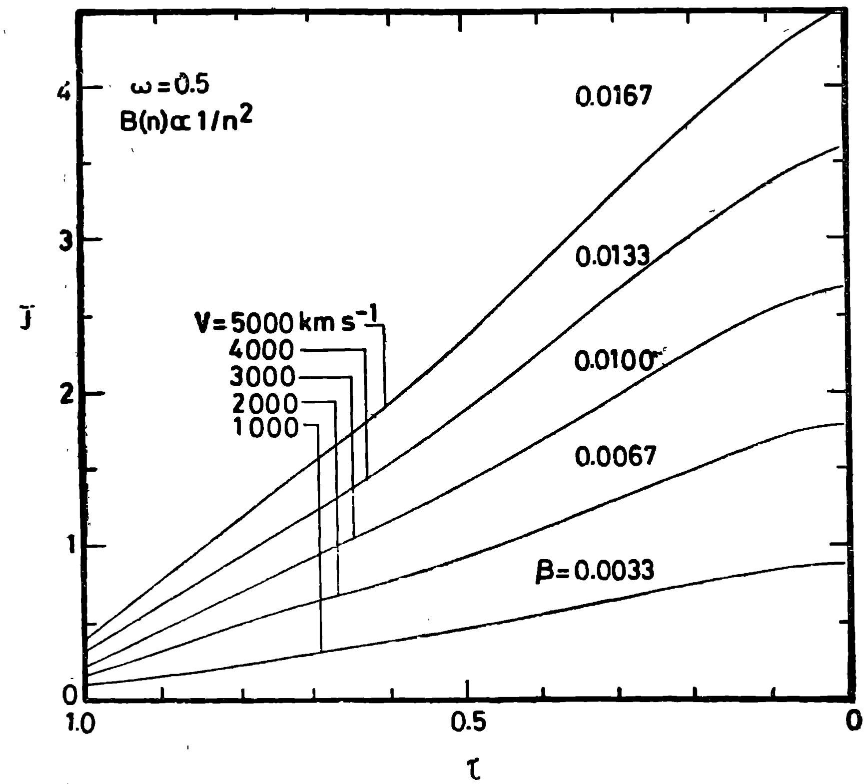

Figure 7. The differences in mean intensities J are plotted for a total optical depth of 1 with Planck function $B(n)$ changing as $1/n^2$.

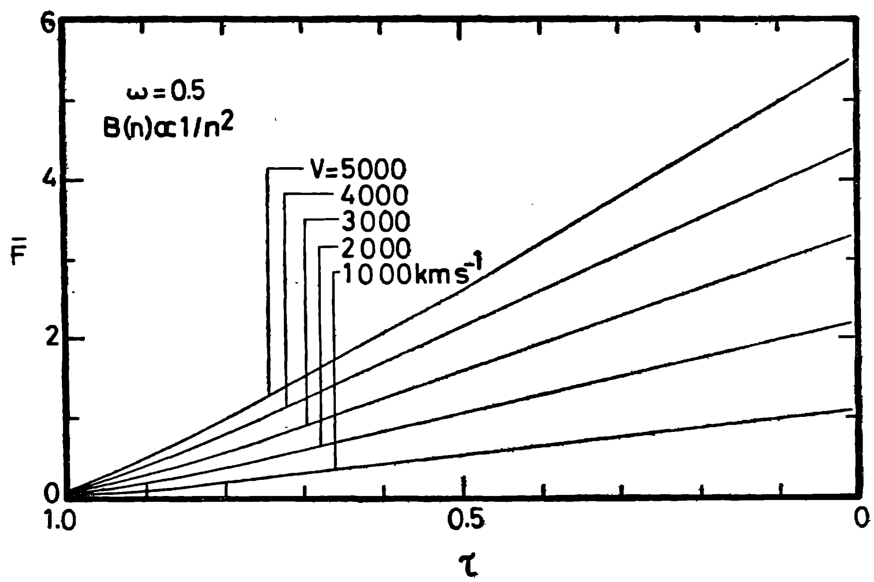

Figure 8. The changes in the outward fluxes are plotted for a total optical depth of 1 with the Planck function $B(n)$ changing as $1/n^2$.

and the optical depth is constant in each layer. The transmission and reflection matrices are calculated for each these layers. By using these quantities we calculated the internal radiation field.

For $\tau = 1$, in figures 1 and 2 we plot the quantities $\bar{J}$ and $\bar{F}$ respectively for different velocities with the Planck function as $B(n) = 1$. For $v = 1000$ km s^{-1}

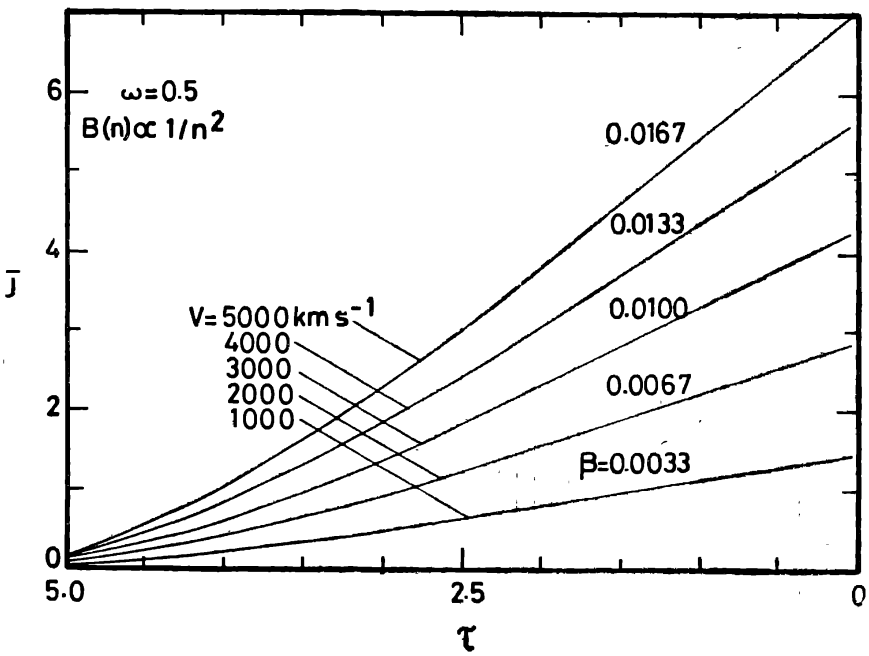

Figure 9. Same as those given in figure 7 for a total optical depth of 5.

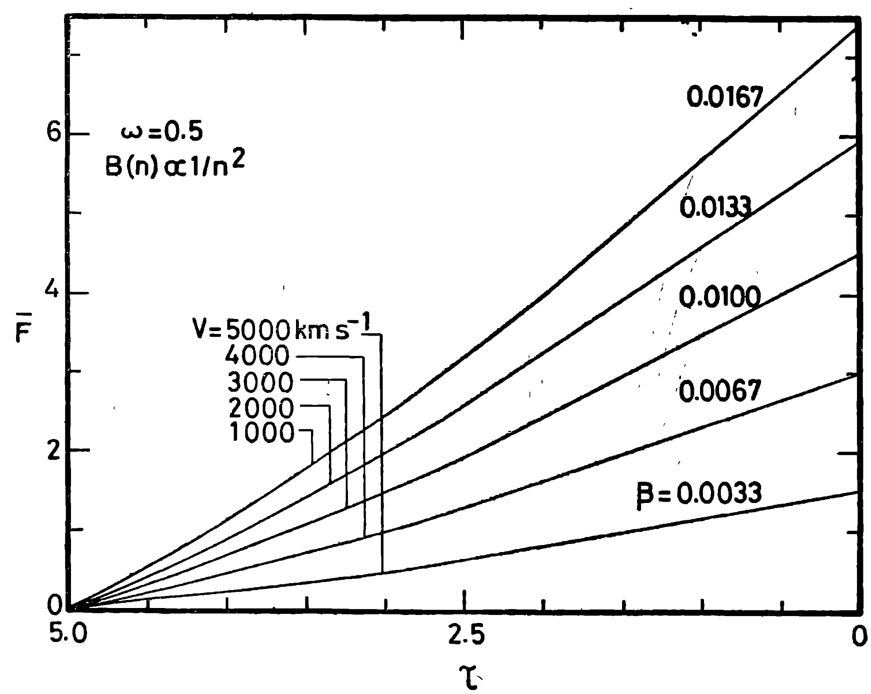

Figure 10. Same as those given in figure 8 for a total optical depth of 5.

($\beta \doteq 0.0033$) the changes are less than 0.5%, but for v = 5000 km s^{-1} ($\beta = 0.0167$) the change is about 2.6%. For a total optical depth of 50 (see figures 3 and 4) $\bar{J}$ and $\bar{F}$ increase to 1.5% and 0.6% respectively. When the optical depth increases, the changes in $\bar{J}$ and $\bar{F}$ are enhanced in the outerlayers.

We plot the amplification factors $\bar{J}_{max}/100\beta$ and $\bar{F}_{max}/100\beta$ versus total thickness of the slab in figures 5 and 6. The amplification factor steeply falls for different velocities with increasing thickness of the plane-parallel slab. This is exactly opposite to the type of variation we notice in paper 1 in which the amplification factor increase with the depth.

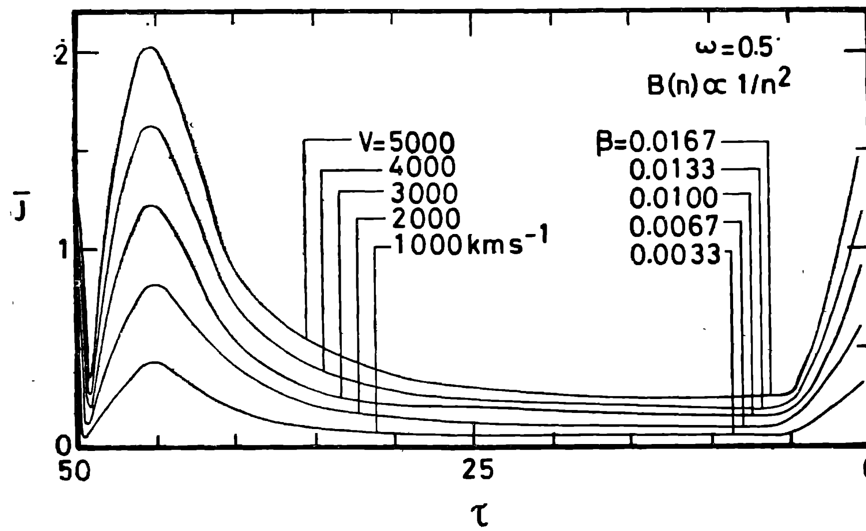

Figure 11. Same as those given in figure 7 for a total optical depth of 50.

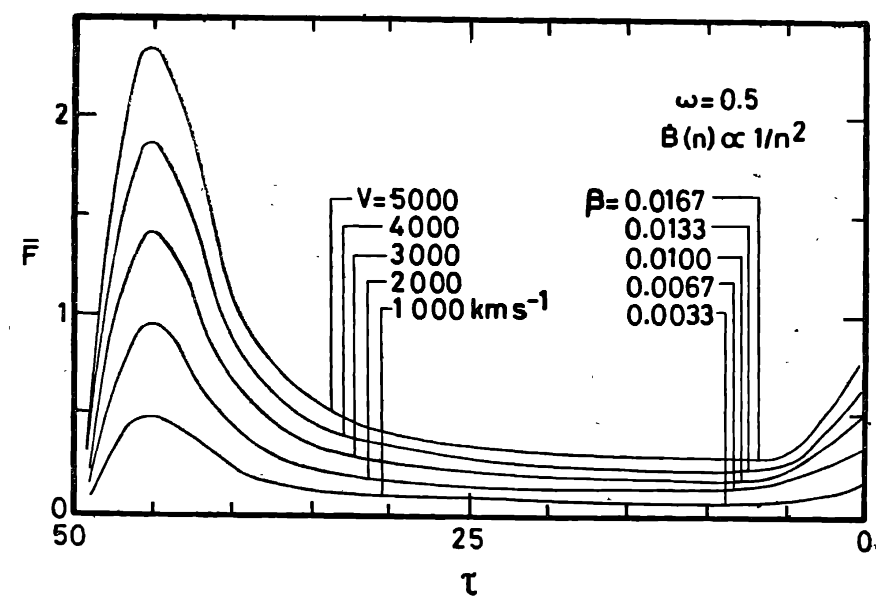

Figure 12. Same as those given in figure 8 in a total optical depth is 50.

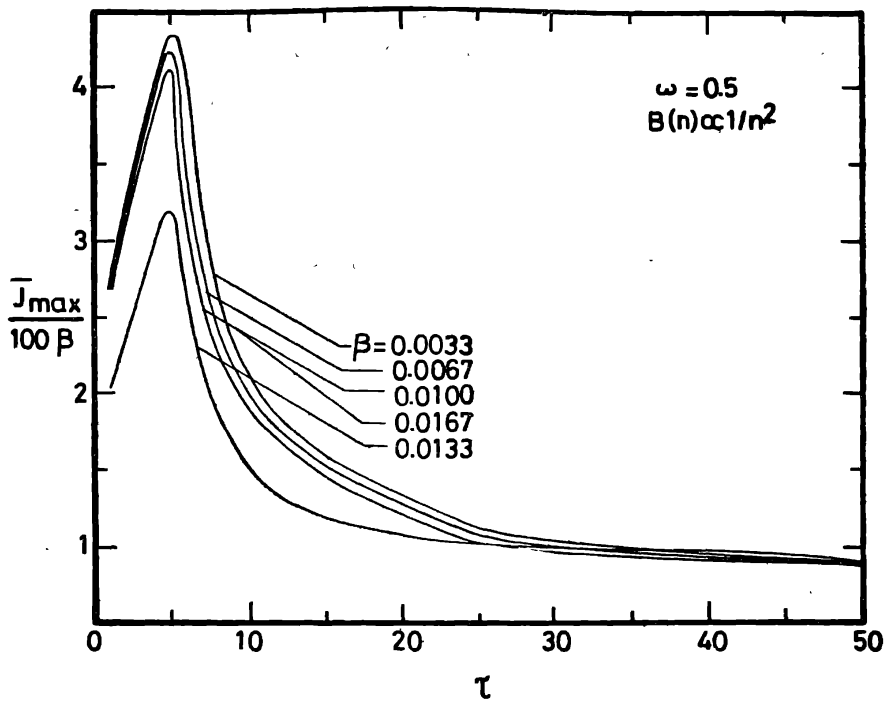

Figure 13. The amplification factor of the difference in mean intensities.

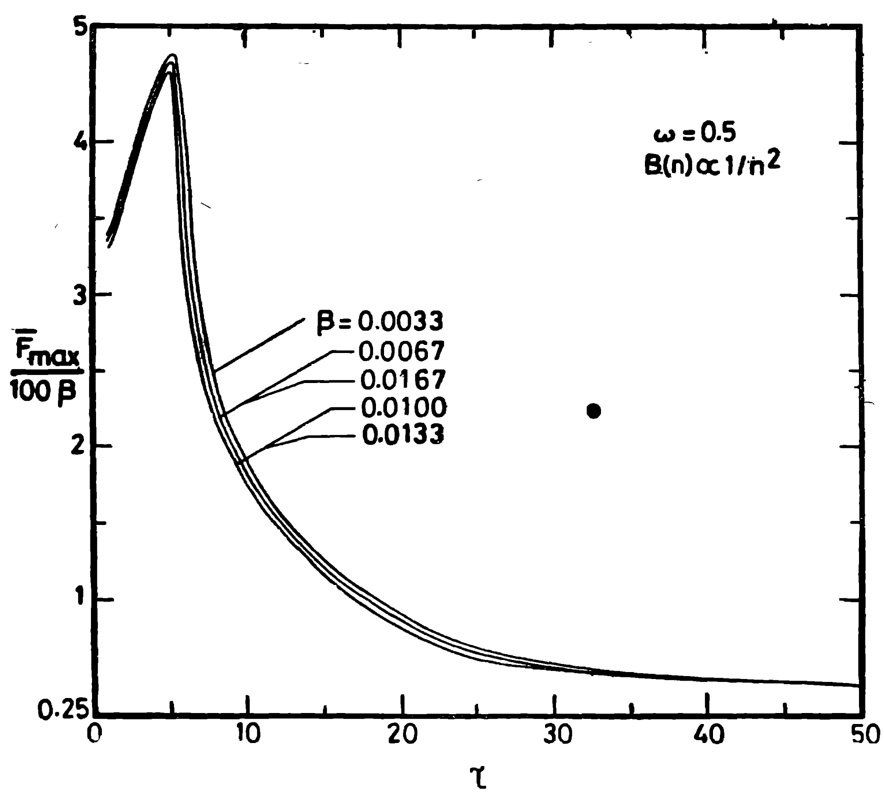

Figure 14. The amplification factors in the difference in outward fluxes.

In figures 7 to 14, we have plotted the changes in $\bar{J}$ and $\bar{F}$ due to aberration and advection for a medium in which the Planck function is changing as $1/n^2$. In figures 7 and 8, $\bar{J}$ and $\bar{F}$ are plotted for $\tau = 1$ for different velocities. The changes are more than those shown in figures 1 and 2. Mean intensity changes by more than 4% while the outward flux changes by about 6%. For an optical depth of 5, the values of $\bar{J}$ and $\bar{F}$ are 6% and 6.5% respectively. However, when τ is increased to 50, $\bar{J}$ and $\bar{F}$ change in a non-monotonic way, maximum being around 2%. The amplification factors fall off rapidly as the depth increases from 1 to 50.

References

Castor, J. H. (1972) *Ap. J.* **178**, 779.

Mihalas, D. (1978) *Stellar atmospheres*, Freeman.

Munier, A. & Weaver, R. (1986) Preprint.

Peraiah, A. (1984) in *Methods in radiative transfer* (ed. : W. Kalkofen) Cambridge Univ. Press, p. 281.

Peraiah, A. (1987) *Ap. J.* **317**, 271 (paper 1).

Peraiah, A. & Varghese, B. A. (1985) *Ap. J.* **290**, 411.